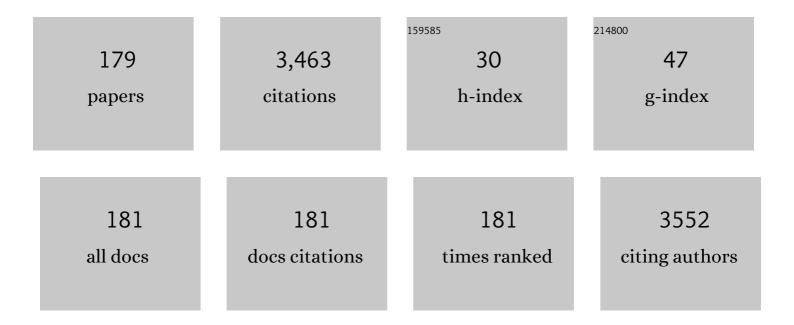
Xiaofeng Li

List of Publications by Year in descending order

Source: https://exaly.com/author-pdf/4366180/publications.pdf Version: 2024-02-01



#	Article	IF	CITATIONS
1	Bridging electromagnetic and carrier transport calculations for three-dimensional modelling of plasmonic solar cells. Optics Express, 2011, 19, A888.	3.4	130
2	Plasmonic Fano resonances in nanohole quadrumers for ultra-sensitive refractive index sensing. Nanoscale, 2014, 6, 4705-4715.	5.6	129
3	Loss mitigation in plasmonic solar cells: aluminium nanoparticles for broadband photocurrent enhancements in GaAs photodiodes. Scientific Reports, 2013, 3, 2874.	3.3	125
4	Multiâ€dimensional modeling of solar cells with electromagnetic and carrier transport calculations. Progress in Photovoltaics: Research and Applications, 2013, 21, 109-120.	8.1	122
5	Planar Hot-Electron Photodetection with Tamm Plasmons. ACS Nano, 2017, 11, 1719-1727.	14.6	115
6	A highly efficient thermo-optic microring modulator assisted by graphene. Nanoscale, 2015, 7, 20249-20255.	5.6	99
7	Photovoltaic Devices: Optoâ€Electroâ€Thermal Physics and Modeling. Advanced Materials, 2017, 29, 1603492.	21.0	87
8	Enhanced Electroâ€Optical Properties of Nanocone/Nanopillar Dualâ€Structured Arrays for Ultrathin Silicon/Organic Hybrid Solar Cell Applications. Advanced Energy Materials, 2016, 6, 1501793.	19.5	75
9	Colored Radiative Cooler under Optical Tamm Resonance. ACS Photonics, 2019, 6, 2545-2552.	6.6	70
10	Radiative cooling of solar cells: opto-electro-thermal physics and modeling. Nanoscale, 2019, 11, 17073-17083.	5.6	66
11	Mismatch Robustness and Security of Chaotic Optical Communications Based on Injection-Locking Chaos Synchronization. IEEE Journal of Quantum Electronics, 2006, 42, 953-960.	1.9	60
12	Modulating oxygen vacancies in Sn-doped hematite film grown on silicon microwires for photoelectrochemical water oxidation. Journal of Materials Chemistry A, 2018, 6, 15593-15602.	10.3	53
13	Thermodynamic loss mechanisms and strategies for efficient hot-electron photoconversion. Nano Energy, 2019, 55, 164-172.	16.0	50
14	Two dimensional graphitic carbon nitride quantum dots modified perovskite solar cells and photodetectors with high performances. Journal of Power Sources, 2020, 451, 227825.	7.8	44
15	Subwavelength focusing behavior of high numerical-aperture phase Fresnel zone plates under various polarization states. Applied Physics Letters, 2009, 95, .	3.3	42
16	High-uniformity multichannel plasmonic filter using linearly lengthened insulators in metal–insulator–metal waveguide. Optics Letters, 2013, 38, 1585.	3.3	42
17	Improving Performance and Stability of Planar Perovskite Solar Cells through Grain Boundary Passivation with Block Copolymers. Solar Rrl, 2019, 3, 1900078.	5.8	40
18	Heterojunction Perovskite Solar Cells: Opto-Electro-Thermal Physics, Modeling, and Experiment. ACS Nano, 2020, 14, 5017-5026.	14.6	40

#	Article	IF	CITATIONS
19	Perovskite Solar Cells: Optoelectronic Simulation and Optimization. Solar Rrl, 2018, 2, 1800126.	5.8	39
20	Enhanced external quantum efficiency in rectangular single nanowire solar cells. Applied Physics Letters, 2013, 102, 021101.	3.3	36
21	Strong and highly asymmetrical optical absorption in conformal metal-semiconductor-metal grating system for plasmonic hot-electron photodetection application. Scientific Reports, 2015, 5, 14304.	3.3	36
22	Scattering effect of the high-index dielectric nanospheres for high performance hydrogenated amorphous silicon thin-film solar cells. Scientific Reports, 2016, 6, 30503.	3.3	36
23	Nanowire and nanohole silicon solar cells: a thorough optoelectronic evaluation. Progress in Photovoltaics: Research and Applications, 2015, 23, 1734-1741.	8.1	35
24	Planar microcavity-integrated hot-electron photodetector. Nanoscale, 2016, 8, 10323-10329.	5.6	35
25	Graphene Plasmon Cavities Made with Silicon Carbide. ACS Omega, 2017, 2, 3640-3646.	3.5	35
26	Optoelectronic modeling of the Si/α-Fe2O3 heterojunction photoanode. Nano Energy, 2018, 43, 177-183.	16.0	34
27	Photonic surface waves enabled perfect infrared absorption by monolayer graphene. Nano Energy, 2018, 48, 161-169.	16.0	33
28	Regulating the Silicon/Hematite Microwire Photoanode by the Conformal Al ₂ O ₃ Intermediate Layer for Water Splitting. ACS Applied Materials & Interfaces, 2019, 11, 5978-5988.	8.0	33
29	Photodetection by Hot Electrons or Hot Holes: A Comparable Study on Physics and Performances. ACS Omega, 2019, 4, 6020-6027.	3.5	33
30	Extremely High Sensitive Plasmonic Refractive Index Sensors Based on Metallic Grating. Plasmonics, 2010, 5, 389-394.	3.4	32
31	Refractive index sensor based on graphene-coated photonic surface-wave resonance. Optics Letters, 2018, 43, 639.	3.3	32
32	High-efficiency photon capturing in ultrathin silicon solar cells with front nanobowl texture and truncated-nanopyramid reflector. Optics Letters, 2015, 40, 1077.	3.3	31
33	Optoelectronic investigation of monolayer MoS2/WSe2 vertical heterojunction photoconversion devices. Nano Energy, 2016, 30, 260-266.	16.0	31
34	Design of low-threshold compact Au-nanoparticle lasers. Optics Letters, 2010, 35, 2535.	3.3	30
35	Broadband enhancement of coaxial heterogeneous gallium arsenide singleâ€nanowire solar cells. Progress in Photovoltaics: Research and Applications, 2015, 23, 628-636.	8.1	29
36	Facile Preparation of <i>n</i> â€Type LaFeO ₃ Perovskite Film for Efficient Photoelectrochemical Water Splitting. ChemistrySelect, 2018, 3, 968-972.	1.5	29

#	Article	IF	CITATIONS
37	Polarization switching of mutually coupled vertical-cavity surface-emitting lasers. Journal of the Optical Society of America B: Optical Physics, 2007, 24, 1276.	2.1	28
38	Infrared hot-carrier photodetection based on planar perfect absorber. Optics Letters, 2015, 40, 4261.	3.3	28
39	Flexible semitransparent perovskite solar cells with gradient energy levels enable efficient tandems with Cu(In,Ga)Se2. Nano Energy, 2020, 78, 105378.	16.0	28
40	Wafer-Scale Integration of Inverted Nanopyramid Arrays for Advanced Light Trapping in Crystalline Silicon Thin Film Solar Cells. Nanoscale Research Letters, 2016, 11, 194.	5.7	27
41	Infrared Nanoimaging Reveals the Surface Metallic Plasmons in Topological Insulator. ACS Photonics, 2017, 4, 3055-3062.	6.6	27
42	Passive and Dynamic Phase-Change-Based Radiative Cooling in Outdoor Weather. ACS Applied Materials & Interfaces, 2022, 14, 14313-14320.	8.0	27
43	Chaos Synchronization and Communication of Cascade-Coupled Semiconductor Lasers. Journal of Lightwave Technology, 2006, 24, 4936-4945.	4.6	26
44	Omnidirectional absorption enhancement of symmetry-broken crescent-deformed single-nanowire photovoltaic cells. Nano Energy, 2015, 13, 9-17.	16.0	26
45	Broadband and wide-angle light harvesting by ultra-thin silicon solar cells with partially embedded dielectric spheres. Optics Letters, 2016, 41, 1329.	3.3	26
46	Broadband Light Harvesting for Highly Efficient Hot-Electron Application Based on Conformal Metallic Nanorod Arrays. ACS Photonics, 2018, 5, 5079-5085.	6.6	26
47	Recent Progress and Future Opportunities for Hot Carrier Photodetectors: From Ultraviolet to Infrared Bands. Laser and Photonics Reviews, 2022, 16, .	8.7	26
48	Planar dual-cavity hot-electron photodetectors. Nanoscale, 2019, 11, 1396-1402.	5.6	24
49	Chaos synchronization of unidirectionally injected vertical-cavity surface-emitting lasers with global and mode-selective coupling. Optics Express, 2006, 14, 3138.	3.4	23
50	Theoretical study on polarization dynamics of VCSELs with negative optoelectronic feedback. Applied Optics, 2007, 46, 7262.	2.1	23
51	Improved optical absorption of silicon single-nanowire solar cells by off-axial core/shell design. Nano Energy, 2015, 17, 233-240.	16.0	23
52	Schottky hot-electron photodetector by cavity-enhanced optical Tamm resonance. Applied Physics Letters, 2017, 110, .	3.3	23
53	Physics and Optoelectronic Simulation of Photodetectors Based on 2D Materials. Advanced Optical Materials, 2019, 7, 1900410.	7.3	23
54	Narrowband and Full-Angle Refractive Index Sensor Based on a Planar Multilayer Structure. IEEE Sensors Journal, 2019, 19, 2924-2930.	4.7	23

#	Article	IF	CITATIONS
55	Surface-plasmon enhanced photodetection at communication band based on hot electrons. Journal of Applied Physics, 2015, 118, .	2.5	22
56	Tunable light absorbance by exciting the plasmonic gap mode for refractive index sensing. Optics Letters, 2018, 43, 1427.	3.3	22
57	Tin and Oxygen-Vacancy Co-doping into Hematite Photoanode for Improved Photoelectrochemical Performances. Nanoscale Research Letters, 2020, 15, 54.	5.7	22
58	Numerical Simulation of Light-Trapping and Photoelectric Conversion in Single Nanowire Silicon Solar Cells. IEEE Journal of Selected Topics in Quantum Electronics, 2013, 19, 1-8.	2.9	21
59	Plasmon gap mode-assisted third-harmonic generation from metal film-coupled nanowires. Applied Physics Letters, 2014, 104, .	3.3	21
60	Silicon-gold core-shell nanowire array for an optically and electrically characterized refractive index sensor based on plasmonic resonance and Schottky junction. Optics Letters, 2017, 42, 1225.	3.3	21
61	Simultaneously performing optical and electrical responses from a plasmonic sensor based on gold/silicon Schottky junction. Optics Express, 2019, 27, 38382.	3.4	21
62	Design of dual-diameter nanoholes for efficient solar-light harvesting. Nanoscale Research Letters, 2014, 9, 481.	5.7	19
63	Experimental demonstration of near-field focusing of a phase micro-Fresnel zone plate (FZP) under linearly polarized illumination. Applied Physics B: Lasers and Optics, 2011, 102, 95-100.	2.2	18
64	Si microwire array photoelectrochemical cells: Stabilized and improved performances with surface modification of Pt nanoparticles and TiO2 ultrathin film. Journal of Power Sources, 2017, 342, 460-466.	7.8	18
65	Tunable infrared hot-electron photodetection by exciting gap-mode plasmons with wafer-scale gold nanohole arrays. Optics Express, 2020, 28, 6511.	3.4	18
66	Nonlinear dynamics of two mutually injected external-cavity semiconductor lasers. Semiconductor Science and Technology, 2006, 21, 25-34.	2.0	16
67	Observation of Tamm plasmon polaritons in visible regime from ZnO/Al2O3 distributed Bragg reflector – Ag interface. Optics Communications, 2011, 284, 1890-1892.	2.1	16
68	Gap-mode excitation, manipulation, and refractive-index sensing application by gold nanocube arrays. Nanoscale, 2019, 11, 5467-5473.	5.6	16
69	Surface plasmonic lasing via the amplification of coupled surface plasmon waves inside dielectric-metal-dielectric waveguides. Optics Express, 2008, 16, 16113.	3.4	15
70	Near-perfect absorber with ultrawide bandwidth in infrared region using a periodically chirped structure. Optics Communications, 2013, 305, 212-216.	2.1	15
71	Self-improvement of solar water oxidation for the continuously-irradiated hematite photoanode. Dalton Transactions, 2019, 48, 15151-15159.	3.3	15
72	Optically injected nanolasers for time-delay signature suppression and communications. Optics Express, 2020, 28, 26421.	3.4	15

#	Article	IF	CITATIONS
73	Theoretical analysis of multi-transverse-mode characteristics of vertical-cavity surface-emitting lasers. Semiconductor Science and Technology, 2005, 20, 505-513.	2.0	14
74	Static and Dynamic Modeling of Circular Grating-Coupled Distributed Feedback Lasers. IEEE Journal of Quantum Electronics, 2008, 44, 770-776.	1.9	14
75	Enhanced photoabsorption in front-tapered single-nanowire solar cells. Optics Letters, 2014, 39, 5756.	3.3	14
76	Plasmonic Filter Using Metal-Insulator-Metal Waveguide with Phase Shifts and its Transmission Characteristics. Plasmonics, 2014, 9, 887-892.	3.4	14
77	Enhanced Photoresponsivity of a Germanium Single-Nanowire Photodetector Confined within a Superwavelength Metallic Slit. ACS Photonics, 2014, 1, 483-488.	6.6	14
78	Stabilized and Improved Photoelectrochemical Responses of Silicon Nanowires Modified with Ag@SiO ₂ Nanoparticles and Crystallized TiO ₂ Film. ACS Applied Materials & Interfaces, 2016, 8, 30072-30078.	8.0	14
79	Random laser action in dielectric-metal-dielectric surface plasmon waveguides. Applied Physics Letters, 2009, 95, 231114.	3.3	13
80	Ultra-broadband performance enhancement of thin-film amorphous silicon solar cells with conformal zig–zag configuration. Optics Letters, 2013, 38, 5071.	3.3	13
81	Size-dependent performances in homogeneous, controllable, and large-area silicon wire array photocathode. Journal of Power Sources, 2020, 473, 228580.	7.8	13
82	Nanobowls-assisted broadband absorber for unbiased Si-based infrared photodetection. Optics Express, 2021, 29, 15505.	3.4	13
83	Suppressing nonlinear dynamics induced by external optical feedback in vertical-cavity surface-emitting lasers. Optics and Laser Technology, 2005, 37, 438-443.	4.6	12
84	Broadband, polarization-insensitive and wide-angle absorption enhancement of a-Si:H/μc-Si:H tandem solar cells by nanopatterning a-Si:H layer. Optics Express, 2013, 21, A677.	3.4	12
85	Design of μc-Si:H/a-Si:H coaxial tandem single-nanowire solar cells considering photocurrent matching. Optics Express, 2014, 22, A1761.	3.4	12
86	Coaxial Ag/ZnO/Ag nanowire for highly sensitive hot-electron photodetection. Applied Physics Letters, 2015, 106, 081109.	3.3	12
87	Design of asymmetric nanovoid resonator for silicon-based single-nanowire solar absorbers. Nano Energy, 2016, 27, 611-618.	16.0	12
88	Facile fabrication of wafer-scale, micro-spacing and high-aspect-ratio silicon microwire arrays. RSC Advances, 2016, 6, 87486-87492.	3.6	12
89	Enhanced Photoelectrical Response of Hydrogenated Amorphous Silicon Single-Nanowire Solar Cells by Front-Opening Crescent Design. Nanoscale Research Letters, 2016, 11, 233.	5.7	12
90	Optoelectronic insights into the photovoltaic losses from photocurrent, voltage, and energy perspectives. AIP Advances, 2017, 7, .	1.3	12

#	Article	IF	CITATIONS
91	Theoretical analysis of graphene plasmon cavities. Applied Materials Today, 2018, 12, 283-293.	4.3	12
92	Planar, narrowband, and tunable photodetection in the near-infrared with Au/TiO ₂ nanodiodes based on Tamm plasmons. Nanoscale, 2019, 11, 23182-23187.	5.6	12
93	Underlayer engineering into the Sn-doped hematite photoanode for facilitating carrier extraction. Physical Chemistry Chemical Physics, 2020, 22, 7306-7313.	2.8	12
94	Nonlinear dynamic behaviors of an optically injected vertical-cavity surface-emitting laser. Chaos, Solitons and Fractals, 2006, 27, 1387-1394.	5.1	11
95	Static and dynamic characteristics of VCSELs with polarisation-selective optical feedback. IEE Proceedings: Optoelectronics, 2006, 153, 67-74.	0.8	11
96	Design and analysis of two-dimensional high-index-contrast grating surface-emitting lasers. Optics Express, 2009, 17, 260.	3.4	11
97	A surface-emitting distributed-feedback plasmonic laser. Applied Physics Letters, 2009, 95, 141114.	3.3	11
98	Absorption enhancement of single silicon nanowire by tailoring rear metallic film for photovoltaic applications. Optics Letters, 2014, 39, 817.	3.3	11
99	Light Trapping Enhancement in a Thin Film with 2D Conformal Periodic Hexagonal Arrays. Nanoscale Research Letters, 2015, 10, 988.	5.7	11
100	Carrier depletion and electrical optimization of gallium arsenide plasmonic solar cell with a rear metallic grating. Applied Physics Letters, 2015, 106, .	3.3	11
101	Nanoparticle mediated microcavity random laser. Photonics Research, 2017, 5, 557.	7.0	11
102	High-Q collective Mie resonances in monocrystalline silicon nanoantenna arrays for the visible light. Fundamental Research, 2023, 3, 822-830.	3.3	11
103	Nonlinear dynamics and localized synchronization in mutually coupled VCSELs. Optics and Laser Technology, 2007, 39, 875-880.	4.6	10
104	Long-wavelength optical transmission of extremely narrow slits via hybrid surface-plasmon and Fabry–Pérot modes. Journal of Applied Physics, 2010, 108, 013302.	2.5	10
105	Limiting efficiency calculation of silicon single-nanowire solar cells with considering Auger recombination. Applied Physics Letters, 2015, 106, .	3.3	10
106	Polarization-insensitive hot-electron infrared photodetection by double Schottky junction and multilayer grating. Optics Letters, 2018, 43, 3325.	3.3	10
107	Photonic Design and Electrical Evaluation of Dual-Functional Solar Cells for Energy Conversion and Display Applications. Nanoscale Research Letters, 2019, 14, 70.	5.7	10
108	Multi-transverse-mode dynamics of vertical-cavity surface-emitting lasers with external optical injection. Journal of the Optical Society of America B: Optical Physics, 2006, 23, 1292.	2.1	9

#	Article	IF	CITATIONS
109	Polarization-resolved dynamics of asymmetrically coupled vertical-cavity surface-emitting lasers. Journal of the Optical Society of America B: Optical Physics, 2008, 25, 153.	2.1	9
110	Stark effect induced microcavity polariton solitons. Optics Express, 2015, 23, 15762.	3.4	9
111	Conformal TCO-semiconductor-metal nanowire array for narrowband and polarization-insensitive hot-electron photodetection application. Journal of Photonics for Energy, 2016, 6, 042502.	1.3	9
112	Polaritonic manipulation based on the spin-selective optical Stark effect in the WS ₂ and Tamm plasmon hybrid structure. Nanoscale, 2019, 11, 4571-4577.	5.6	9
113	Synergistic engineering of bromine and cetyltrimethylammonium chloride molecules enabling efficient and stable flexible perovskite solar cells. Journal of Materials Chemistry A, 2020, 8, 19425-19433.	10.3	9
114	Managing Lead Leakage in Efficient Perovskite Solar Cells with Phosphate Interlayers. Advanced Materials Interfaces, 0, , 2200570.	3.7	9
115	Design and analysis of a surface plasmon polariton modulator using the electro-optic effect. Applied Optics, 2009, 48, 6600.	2.1	8
116	Quarter-wave plate with subwavelength rectangular annular arrays. Optics Communications, 2013, 297, 198-203.	2.1	8
117	A new method for measuring wetness of flowing steam based on surface plasmon resonance. Nanoscale Research Letters, 2014, 9, 18.	5.7	8
118	Ambipolar Self-Driving Polarized Photodetection. ACS Photonics, 2021, 8, 2459-2465.	6.6	8
119	Modal characteristics of terahertz surface-emitting distributed-feedback lasers with a second-order concentric-circular metal grating. Journal of Applied Physics, 2009, 106, 053103.	2.5	7
120	Enhanced Photoelectrochemical Response of Silicon Nanowire Arrays through Coating the Carbon Shell. Journal of the Electrochemical Society, 2014, 161, H240-H243.	2.9	7
121	Core–Shell Singleâ€Nanowire Photodetector with Radial Carrier Transport: an Opportunity to Break the Responsivity‧peed Tradeâ€off. Advanced Electronic Materials, 2021, 7, 2000920.	5.1	7
122	Passive radiative temperature regulator: Principles and absorption-emission manipulation. Solar Energy Materials and Solar Cells, 2021, 229, 111143.	6.2	7
123	Selfâ€Driving Perovskite Dember Photodetectors. Advanced Optical Materials, 2022, 10, 2101821.	7.3	7
124	Efficient Flexible Perovskite Solar Cells with Reduced Hysteresis Employing Cobalt Nitrate Treated SnO ₂ . Solar Rrl, 2022, 6, .	5.8	7
125	2D MXenes for Hotâ€Carrier Photodetection. Advanced Optical Materials, 2022, 10, .	7.3	7
126	Effects of unwanted feedback on synchronized chaotic optical communications. Applied Optics, 2006, 45, 2510.	2.1	6

#	Article	IF	CITATIONS
127	Reflective plasmonic waveplates based on metal–insulator–metal subwavelength rectangular annular arrays. Photonics and Nanostructures - Fundamentals and Applications, 2014, 12, 189-198.	2.0	6
128	Synthetic Plasmonic Nanocircuits and the Evolution of Their Correlated Spatial Arrangement and Resonance Spectrum. ACS Photonics, 2021, 8, 166-174.	6.6	6
129	Singleâ€Shot Interaction and Synchronization of Random Microcavity Lasers. Advanced Materials Technologies, 2021, 6, 2100562.	5.8	6
130	Diffraction Characteristics of Concentric Circular Metal Grating Operating at Terahertz Regime. IEEE Journal of Quantum Electronics, 2010, 46, 898-905.	1.9	5
131	An Index-Guided ZnO Random Laser Array. IEEE Photonics Technology Letters, 2011, 23, 522-524.	2.5	5
132	Performance-improved thin-film a-Si:H/μc-Si:H tandem solar cells by two-dimensionally nanopatterning photoactive layer. Nanoscale Research Letters, 2014, 9, 73.	5.7	5
133	Perovskite Solar Cells: Optoelectronic Simulation and Optimization (Solar RRL 11â^•2018). Solar Rrl, 2018, 2, 1870227.	5.8	5
134	Energy Tracing of Photovoltaic Cells. Solar Rrl, 2021, 5, 2100199.	5.8	5
135	Polarization switching and synchronization of mutually coupled vertical-cavity surface-emitting semiconductor lasers. Chinese Physics B, 2007, 16, 1996-2002.	1.3	4
136	Proximity effect assisted absorption enhancement in thin film with locally clustered nanoholes. Optics Letters, 2015, 40, 792.	3.3	4
137	Vibration detection schemes based on absorbance tuning in monolayer molybdenum disulfide mechanical resonators. 2D Materials, 2019, 6, 011003.	4.4	4
138	Single-nanowire silicon photodetectors with core-shell radial Schottky junction for self-powering application. Applied Physics Letters, 2021, 118, .	3.3	4
139	Characterizing the chaotic dynamics of a semiconductor nanolaser subjected to FBG feedback. Optics Express, 2021, 29, 17815.	3.4	4
140	Direct growth of hematite film on p+n-silicon micro-pyramid arrays for low-bias water splitting. Solar Energy Materials and Solar Cells, 2021, 224, 110987.	6.2	4
141	Easy-to-process and high-performance colorful perovskite solar cells using a multilayer planar filter. Optics Letters, 2020, 45, 6326.	3.3	4
142	Enhancing Hot-Electron Photodetection of a TiO2/Au Schottky Junction by Employing a Hybrid Plasmonic Nanostructure. Materials, 2022, 15, 2737.	2.9	4
143	Photo-assisted decoration of Ag-Pt nanoparticles on Si photocathodes for reducing overpotential toward enhanced photoelectrochemical water splitting. Science China Materials, 2022, 65, 3033-3042.	6.3	4
144	Influence of polarization-selected mutual injection on the polarization-switching dynamics of vertical-cavity surface-emitting lasers. Journal of the Optical Society of America B: Optical Physics, 2007, 24, 2472.	2.1	3

#	Article	IF	CITATIONS
145	ZnO–ZnMgO Multiple Quantum-Well Ridge Waveguide Lasers. IEEE Photonics Technology Letters, 2009, 21, 1624-1626.	2.5	3
146	Excitation and Optimization Modeling of Surface Plasmon Polaritons in a Concentric Circular Metallic Grating Film. Plasmonics, 2010, 5, 69-74.	3.4	3
147	Hybrid Solar Cells: Enhanced Electroâ€Optical Properties of Nanocone/Nanopillar Dualâ€Structured Arrays for Ultrathin Silicon/Organic Hybrid Solar Cell Applications (Adv. Energy Mater. 8/2016). Advanced Energy Materials, 2016, 6, .	19.5	3
148	Manipulating the directional emission of monolayer semiconductors by dielectric nanoantenna arrays. Journal of Optics (United Kingdom), 2022, 24, 024005.	2.2	3
149	Back Interface Passivation for Efficient Low-Bandgap Perovskite Solar Cells and Photodetectors. Nanomaterials, 2022, 12, 2065.	4.1	3
150	Multiple-Mode Behavior of Circular-Grating-Coupled Distributed Feedback Lasers. Journal of Lightwave Technology, 2008, 26, 3345-3354.	4.6	2
151	Modeling of Rabi splitting in quantum well microcavities using time-dependent transfer matrix method. Optics Express, 2008, 16, 19285.	3.4	2
152	Suppression of Random Lasing Modes in Polycrystalline ZnO Thin-Film by Using Distributed Bragg Reflector. IEEE Photonics Technology Letters, 2009, 21, 549-551.	2.5	2
153	Enhanced Light Trapping in a-Si:H/μc-Si:H Tandem Solar Cells via Nanopatterning Top Absorber and Embedding Wavelength-Selective Intermediate Reflectors. IEEE Journal of Photovoltaics, 2015, 5, 46-54.	2.5	2
154	The Role of Master Laser with Feedback in Time-Delay Signature Suppression of Semiconductor Laser Subject to Chaotic Optical Injection. International Journal of Bifurcation and Chaos in Applied Sciences and Engineering, 2017, 27, 1750169.	1.7	2
155	Physical manipulation of ultrathin-film optical interference for super absorption and two-dimensional heterojunction photoconversion. Chinese Physics B, 2018, 27, 124202.	1.4	2
156	Control of nonlinear dynamics in external-cavity VCSELs with delayed negative optoelectronic feedback. Chaos, Solitons and Fractals, 2006, 30, 1004-1011.	5.1	1
157	Analysis and Design of Antiresonant Reflecting Optical Waveguide Vertical-Cavity Surface-Emitting Lasers for Above-Threshold Operation. Journal of Lightwave Technology, 2008, 26, 1935-1942.	4.6	1
158	Design of Stable Single-Mode Chaotic Light Source Using Antiresonant Reflecting Optical Waveguide Vertical-Cavity Surface-Emitting Lasers. IEEE Journal of Quantum Electronics, 2008, 44, 338-345.	1.9	1
159	Highly efficient ultra-thin crystalline silicon solar cell with plasmonic cavities. International Journal of Nanotechnology, 2015, 12, 769.	0.2	1
160	Enhanced light-harvesting capability for silicon single-nanowire solar cells coupled with metallic cavity. Optics Express, 2016, 24, A1505.	3.4	1
161	Investigation on the Strong Light-Matter Interaction in the Graphene-Perovskite Heterostructure Photodetector. Materials Science Forum, 0, 926, 85-91.	0.3	1
162	Opto-electro-thermal simulation technology of solar cells. Journal of Semiconductors, 2019, 40, 050403.	3.7	1

#	Article	IF	CITATIONS
163	Energy Tracing of Photovoltaic Cells. Solar Rrl, 2021, 5, 2170072.	5.8	1
164	Planar Narrowband Hot-Electron Photodetector Based on Tamm Plasmons. , 2019, , .		1
165	Low Band Gap Perovskite Concentrator Solar Cells: Physics, Device Simulation, and Experiment. ACS Applied Materials & Interfaces, 2022, 14, 29856-29866.	8.0	1
166	High performance of hot-carrier generation, transport and injection in TiN/TiO2 junction. Frontiers of Physics, 2022, 17, .	5.0	1
167	Aluminum Nanoparticles for Efficient Light-trapping in Plasmonic Gallium Arsenide Solar Cells. , 2012, , .		Ο
168	Al nanoparticle arrays for broadband absorption enhancements in GaAs devices. , 2013, , .		0
169	Study on limiting efficiencies of a-Si:H/μc-Si:H-based single-nanowire solar cells under single and tandem junction configurations. Applied Physics Letters, 2015, 107, 181106.	3.3	Ο
170	Polarization-dependent excitation of Tamm plasmon and surface plasmon in one hybrid optical structure. , 2016, , .		0
171	Optoelectronic design on the hot-carrier photodetectors. , 2016, , .		0
172	Optoelectronic and thermodynamic simulation of solar cells. , 2016, , .		0
173	Plasmonics and Antenna Effect Mediated Super Absorption in Ultrathin Film via Core/Shell Design. IEEE Photonics Technology Letters, 2017, 29, 893-896.	2.5	0
174	Multiscale evaluation of microscopic stitching with tilt compensation based on metal engineering surfaces. Measurement: Journal of the International Measurement Confederation, 2021, 176, 109183.	5.0	0
175	Planar Dual-Layer System for Ultra-Broadband Absorption and Hot-Carrier Photodetection in Longwave Near-Infrared Band. IEEE Journal of Selected Topics in Quantum Electronics, 2022, 28, 1-9.	2.9	0
176	3D device simulation of plasmonic solar cells. , 2012, , .		0
177	Influences of Metal Nanoparticles on the Photoelectrochemical Activity of Silicon Nanowires for Photon Harvesting. , 2015, , .		0
178	A complete simulation of nanostructured solar cells considering absorption and photoconversion processes. , 2015, , .		0
179	Optoelectronic and Thermodynamic Study of Solar Cells. , 2016, , .		0